The Dynamics of Electron Self-Exchange between Nanoparticles

Jocelyn F. Hicks, Francis P. Zamborini, Andrea J. Osisek,† and Royce W. Murray*

Contribution from the Kenan Laboratories of Chemistry, University of North Carolina, CB#3290, Chapel Hill, North Carolina 27599-3290

Received March 14, 2001

Abstract: The rate of electron self-exchange reactions between discretely charged metal-like cores of nanoparticles has been measured in multilayer films of nanoparticles by an electrochemical method. The nanoparticles are Au monolayer-protected clusters with mixed monolayers of hexanethiolate and mercaptoundecanoic acid ligands, linked to each other and to the Au electrode surface with carboxylate−metal ion−carboxylate bridges. Cyclic voltammetry of the nanoparticle films exhibits a series of well-defined peaks for the sequential, single-electron, double-layer charging of the 1.6-nm-diameter Au cores. The electron self-exchange is measured as a diffusion-like electron-hopping process, much as in previous studies of redox polymer films on electrodes. The average electron diffusion coefficient is $D_E = 10(\pm 5) \times 10^{-8}$ cm^2/s, with no discernible dependence on the state of charge of the nanoparticles or on whether the reaction increases or decreases the core charge. This diffusion constant corresponds to an average first-order rate constant k_{HOP} of $2(\pm 1) \times 10^6$ s^{-1} and an average self-exchange rate constant, k_{EX}, of $2(\pm 1) \times 10^8$ M^{-1} s^{-1}, using a cubic lattice hopping model. This is a very large rate constant, considering the nominally lengthy linking bridge between the Au cores.

Introduction

Nanoparticles that we call monolayer-protected gold clusters (MPCs) are nanometer-scale gold particles coated with a dense, protecting monolayer of thiolate ligands. The chemically vital aspect of an MPC is the stability afforded by the monolayer protection of the core and the consequent ability to design and manipulate the monolayer's functionality.[1] We have discovered[2] that the double-layer capacitances (C_{CLU}) of alkanethiolate-protected MPCs are so small (sub-attofarad) that room-temperature resolution of single-electron charging events becomes possible, i.e., the voltage intervals (ΔV) between successive one-electron charging steps of the MPC cores are $> k_BT$, and can be voltammetrically resolved on the potential axis.[2−4] This phenomenon occurs with the MPC bathed in electrolyte solution and is dubbed quantized double-layer charging (QDL).[2−4] QDL is observed both for MPCs dissolved[2−4] in electrolyte solutions and diffusing to the electrode, or attached to the electrode as monolayers[5] or multilayers.[6] The MPC capacitances C_{CLU} are approximately the same in these circumstances. Observing QDL requires that the MPCs are reasonably monodisperse (or have a dominant population) in core size and thus in C_{CLU} and ΔV.

The thermodynamics of quantized double-layer charging has been outlined in previous work.[2,3,7] The capacitance C_{CLU} and associated spacing ΔV between successive one-electron double-layer charging steps of MPCs depend on the Au core size and the monolayer thickness and dielectric constant. The voltage spacing is less dependent on the solvent[4] and can depend on the electrolyte ions.[8] The state of charge of the MPC core is reckoned from the MPC's potential of zero charge.[7b]

Much less is known about the *dynamics* of electron-transfer reactions of metal nanoparticles, including MPCs, whether the reaction is nanoparticle−nanoparticle or nanoparticle−electrode or nanoparticle−redox moiety, either in solution or surface-attached. The chemistry of electron-transfer kinetics between tiny ligand-stabilized pieces of metal is a fascinating prospect with some fundamental importance. We have recently[9] reported on the rates of bimolecular electron transfers between MPCs in their mixed-valent solids. The rate constants are exponentially dependent on the protecting (and MPC core-separating) alkanethiolate chain length and are very large, in the range of ca. 10^9−10^{11} M^{-1} s^{-1}. Another report[10] has claimed to measure the rate of electron transfers between an electrode and a monolayer of MPCs. Related reports are STM-based experiments measuring single-molecule resistances[11] and the resistances of monolayers[12] on nanoparticles. Further generic approaches for study of nanoparticle electron-transfer dynamics would be valuable.

† Current address: Department of Chemistry, Shippensburg University, 1871 Old Main Dr., Shippensburg, PA 17257-2299.

(1) Templeton, A. C.; Wuelfing, W. P.; Murray, R. W. *Acc. Chem. Res.* **2000**, *33*, 27−36.

(2) Ingram, R. S.; Hostetler, M. J.; Pietron, J. J.; Murray, R. W.; Schaaff, T. G.; Khoury, J.; Whetten, R. L.; Bigioni, T. P.; Guthrie, D. K.; First, P. N. *J. Am. Chem. Soc.* **1997**, *119*, 9279.

(3) Chen, S.; Ingram, R. S.; Hostetler, M. J.; Pietron, J. J.; Murray, R. W.; Schaaff, T. G.; Khoury, J.; Alvarez, M. M.; Whetten, R. L. *Science* **1998**, *280*, 2098.

(4) Hicks, J. F.; Templeton, A. C.; Chen, S.; Sheran, K. M.; Jasti, R.; Murray, R. W.; Debord, J.; Schaaff, T. G.; Whetten, R. L. *Anal. Chem.* **1999**, *71*, 3703.

(5) Hicks, J. F.; Zamborini, F. P.; Murray, R. W., manuscript in prepartion.

(6) Zamborini, F. P.; Hicks, J. F.; Murray, R. W. *J. Am Chem. Soc.* **2000**, *122*, 4515.

(7) (a) Chen, S.; Murray, R. W.; Feldberg, S. W. *J. Phys. Chem. B* **1998**, *102*, 9898. (b) Chen, S.; Murray, R. W. *J. Phys. Chem. B* **1999**, *103*, 9996.

(8) Chen, S. *Langmuir* **1999**, *15*, 7551.

(9) Wuelfing, W. P.; Green, S. J.; Cliffel, D. E.; Pietron, J. P.; Murray, R. W. *J. Am. Chem. Soc.* **2000**, *122*, 11465.

(10) Chen, S. *J. Phys. Chem.* **2000**, *104*, 663.

(11) (a) Chen, J.; Reed, M. A.; Asplund, C. L.; Cassell, A. M.; Myrick, M. L.; Rawlett, A. M.; Tour, J. M.; Van Patten, P. G. *Appl. Phys. Lett.* **1999**, *75*, 624. (b) Reed, M. A.; Zhou, C.; Muller, C. J.; Burgin, T. P.; Tour, J. M. *Science* **1997**, *278*, 252.

(12) Bigioni, T. P.; Harrell, L. E.; Guthrie, D. K.; Cullen, W. G.; Whetten, R. L.; First, P. N. *Eur. Phys. J.* **1999**, *D6*, 355.

10.1021/ja0106826 CCC: $20.00
Published on Web 06/30/2001

Scheme 1. Cartoon Showing Multilayers of Au (C6/C10COOH) MPCs Assembled on a MUA-Functionalized Au Electrode[a]

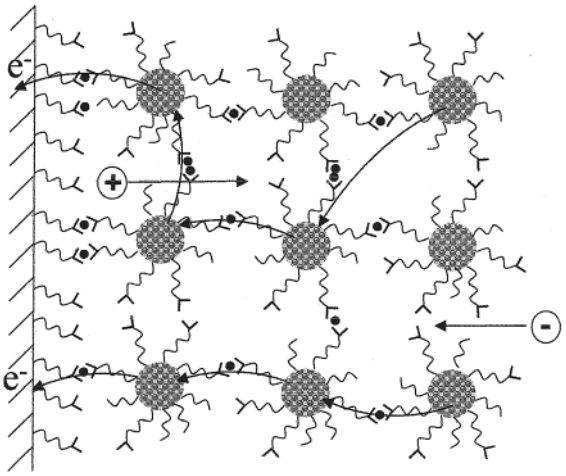

[a] MPCs are linked to the electrode surface and each other through a carboxylate−metal ion−carboxylate bridge. Arrows depict possible pathways for electron movement through the film. Counterion movement is vaguely depicted as the positive and negative flow of charge into and out of the film, so as to satisfy electroneutrality.

We recently described[6] how to assemble multilayer films of MPCs with mixed monolayers (alkanethiolate and carboxyalkanethiolate ligands) on electrodes. Voltammetry of these films showed that the quantized double-layer charging of MPCs can be recognizably propagated throughout the entire nanoparticle film, i.e., the rate of electron self-exchange between nanoparticles was comparable to the experimental time scale. This observation offered a general pathway to measurements of such rates that is analogous to well-known[13,14] tactics for measuring electron-hopping rates in films of redox polymers. A change in electrode potential initiating a redox reaction at the electrode/polymer interface is followed by a sequence of electron-hopping reactions that proceeds further into the film of redox polymer until the film is exhaustively oxidized or reduced. Discretized double-layer charging (QDL) in the MPC films is equivalent to redox oxidation or reduction in the polymer films. The electron hopping follows diffusion principles, so that standard electrochemical methods can be deployed to determine the electron diffusion coefficient, D_E. The analogy to the nanoparticle film's oxidation is that quantized double-layer charging (QDL) is a pseudo-redox process that allows identification of the state of charge of the nanoparticle core.[2−4,7]

This paper will show for the first time that the diffusion-like electron transport in multilayer films can be used to extract nanoparticle−nanoparticle electron-transfer dynamics. Scheme 1 illustrates the electron diffusion measurement, where a change in electrode potential moves the Fermi level of the nanoparticles to more positive values, corresponding to a positive charge state change on the MPC cores. The charge state change is initiated at the electrode/nanoparticle interface and propagates outward into the bulk of the MPC film, until the entire film comes into equilibrium with the applied potential. The rate of the diffusion-like electron hopping is measured using a potential step method, chronoamperometry,[15] a standard method for electron diffusion in redox polymers.[13,14] D_E is related to the rate of electrons hopping between (we assume only between nearest-neighbor) MPC cores using a (fictitious) cubic lattice model,

$$D_E = k_{HOP}\delta^2/6 = k_{EX}\delta^2 C/6 \quad (1)$$

where k_{HOP} and k_{EX} are rate constants of electron transfer expressed as first (s^{-1}) and second-order ($M^{-1}\ s^{-1}$) processes, respectively. In this model, δ is the equilibrium center−center core separation (and thus the effective length of the electron hop) and C is the concentration of MPC cores in the nanoparticle film. Scheme 2 depicts (roughly to scale) the carboxylate−metal ion−carboxylate bridge. The long linker bridge was used to slow the electron-hopping rate to an experimentally accessible range, and to facilitate the mobility of charge-compensating counterions throughout the MPC film.

Scheme 2. Cartoon Depicting MPCs Linked Together via a Carboxylate−Metal Ion−Carboxylate Bridge

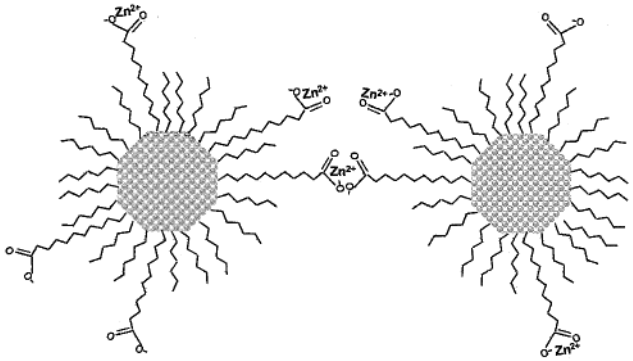

It is worth noting that, in principle, the monolayers on MPCs diffusing to and undergoing electron charging at naked electrodes should also retard their electron transfers so that their charging rates could be measured. In the observed QDLs of diffusing MPCs, this has not been a productive avenue, because monodisperse MPCs with monolayer tunneling barriers of sufficient thickness to yield measurable electron-transfer rates are not easily accessible. MPCs with hexanethiolate monolayers and with reasonable core monodispersity are accessible, but C6 monolayers do not offer a thus-far observable resistance to charge transfer (relative to diffusional transport resistance).

Experimental Section

Synthesis of Mixed Monolayer MPCs. Monolayer-protected clusters (MPCs) with hexanethiolate (C6) monolayers were prepared using a modified Brust[16] synthesis. Briefly, the thiol and $AuCl_4^-$ were combined in a 3:1 mole ratio in toluene, and a 10-fold excess of reductant ($NaBH_4$ in water) was added at 0 °C. The MPC product was recovered from the stirred reaction mixture after 24 h by precipitation, filtering, and thorough washing with acetonitrile on a glass fritted Buchner funnel. This MPC product, which has an average core mass of 28 kDa according to laser desorption−ionization mass spectrometry,[4,17] is denoted C6 MPC. Mercaptoundecanoic acid ($HS(CH_2)_{10}CO_2H$, MUA) was incorporated into the MPC monolayer by ligand place-exchange,[18] stirring tetrahydrofuran (THF) solutions of MPC and the MUA thiol (in selected molar ratios) for ca. 4 days. The mixed-monolayer MPC product was collected and washed as above. The mole ratio of C6 and MUA thiolates in the mixed monolayer MPC was determined by NMR of solutions of the disulfides that are quantitatively

(13) Majda, M. In *Molecular Design of Electrode Surfaces*; Murray, R. W., Ed.; John Wiley and Sons: New York, 1992.
(14) Daum, P.; Murray, R. W. *J. Phys. Chem.* **1981**, *85*, 389.
(15) Bard, A. J.; Faulkner, L. R. *Electrochemical Methods*; Wiley: New York, 2000.
(16) Brust, M.; Walker, M.; Bethell, D.; Schiffrin, D. J.; Whyman, R. *Chem. Commun.* **1994**, 801.
(17) Whetten, R. L.; Khoury, J. T.; Alvarez, M. M.; Murthy, S.; Vezmar, I.; Wang, Z. L.; Stephens, P. W.; Cleveland, C. L.; Luedtke, W. D.; Landman, U. *Adv. Mater.* **1996**, *8*, 428.
(18) Hostetler, M. J.; Templeton, A. C.; Murray, R. W. *Langmuir* **1999**, *15*, 3782.

liberated from mixed-monolayer MPCs upon decomposition with iodine.[19] In the place-exchange reaction, the product MPC had a mixed monolayer with a ratio of MUA and C6 ligands that was roughly one-half of the ratio of MUA thiol and C6 MPC thiolate ligands present in the exchange solution.

Based on TEM and thermogravimetry done as described previously,[18] the MPCs had an *average* composition of $Au_{140}(C6)_{53}$ prior to place exchange, and based on NMR after the place exchange, they had an *average* composition of $Au_{140}(MUA)_{20}(C6)_{33}$. The compositions are average in that a dispersion of Au core sizes exists (as determined by TEM) and that some dispersity in the MUA/C6 ligand ratio is statistically expected over the MPC population. The population of Au_{140} MPC cores is sufficiently dominant in both the parent $Au_{140}(C6)_{53}$ and place-exchanged $Au_{140}(MUA)_{20}(C6)_{33}$ materials that quantized double-layer charging peaks appear in their solution voltammetry, and in that of surface-attached[6] $Au_{140}(MUA)_{20}(C6)_{33}$. The samples are not, however, entirely monodisperse, and nanoparticles with a range of MPC capacitances appear as a double-layer charging current that is featureless on the potential axis.

Self-Assembled Monolayer (SAM) Formation. MUA monolayers on Au electrodes were formed by placing a Au disk electrode (Bioanalytical Systems, 0.02 cm^2 area) in a 2 mM ethanol solution of MUA for at least 24 h. The Au electrode had been polished with 0.25-μm diamond paste (Buehler), rinsed with distilled and NANOpure water, and cleaned by cycling between potentials of −1.2 and 0.4 V vs SCE at 1 V/s in sulfuric acid for ca. 3 min.[15]

Attachment of MPCs to Electrodes. The MPC film was formed[6] by first deprotonating and then metalating the MUA monolayer on the Au electrode with 1 mM KOH in ethanol (EtOH, 20 min) and 0.2 M $Zn(NO_3)_2$ in EtOH (20 min), respectively. This surface was exposed to a 70 μM solution of the mixed monolayer $Au_{140}(MUA)_{20}(C6)_{33}$ MPCs in EtOH (containing a small amount of KOH) for 45 min. The electrode is rinsed with ethanol between these steps to remove any material not strongly bound to its surface. This sequence of steps, i.e., a dipping cycle, under the specified conditions attaches roughly 10 monolayers of MPCs to the electrode surface. The attained MPC film coverage can be monitored[20] by using its quantized double-layer charging voltammetry or, alternatively, from the optical absorbance of films grown similarly on glass slides.[20b] Approximately a single MPC monolayer (ca. 2×10^{-11} mol/cm^2)[20c] can be attached by decreasing the time the electrode is exposed to the MPC solution to ca. 3−5 min, as for example was done in the first dipping cycle in Figure 1A, curve 2.

Electrochemical Measurements. Cyclic voltammetry (CV) and chronoamperometry of the MPC films on Au electrodes were performed with a Bioanalytical Systems 100B electrochemical analyzer, in 0.1 M Bu_4NPF_6/CH_2Cl_2 electrolyte solutions, in a single compartment cell containing a Pt flag counter and a $Ag/AgNO_3$ reference electrode. Background scans were obtained on the MUA-modified Au electrode, prior to MPC attachment, to confirm, by a small charging current, that a well-ordered MUA SAM was present.

Results

Electron-Transfer Dynamics in Multilayer MPC Films. Cyclic voltammograms are shown in Figure 1 that result from a series of dipping cycles (Experimental Section) forming multilayers of carboxylate/Zn^{2+}/carboxylate-linked $Au_{140}(MUA)_{20}(C6)_{33}$ films. Curve 1 is the MUA SAM. Curve 2 corresponds to roughly one monolayer of attached MPCs (ca. 3×10^{-11} mole/cm^2). Curves 3−6 display the responses of MPC films produced by multiple dipping cycles that, by comparison to curve 2, contain the equivalent of many monolayers of nanoparticles. Trials produced experimental guidelines under which electron diffusion could be measured for films that attained (total) peak currents of ~4 μA (at a scan rate of 50 mV/s), like those in curves 5 and 6.

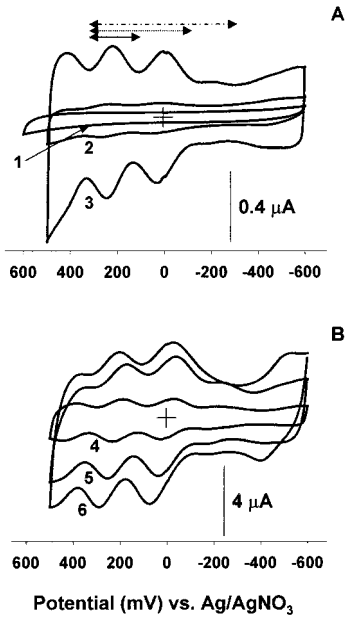

Figure 1. Cyclic voltammograms depicting MPC film growth with multiple dipping cycles all at 50 mV/s scan rate, 0.1 M Bu_4NPF_6 in CH_2Cl_2, potential vs $Ag/AgNO_3$ reference, 0.02 cm^2 working electrode area, Pt flag counter electrode. (Panel A) Curve 1, MUA; curve 2, first dipping cycle [coverage = 3×10^{-11} mol/cm^2 (~1 monolayer)]; curve 3, second dipping cycle [coverage = 1.6×10^{-10} mol/cm^2 (~8 monolayers)]. (Panel B) Curve 4, third dipping cycle [coverage = 3.1×10^{-10} mol/cm^2 (~16 monolayers)]; curve 5, fourth dipping cycle [coverage = 6.2×10^{-10} mol/cm^2 (~31 monolayers)]; curve 6, sixth dipping cycle [coverage = 1.1×10^{-9} mol/cm^2 (~55 monolayers)]. Coverage was estimated using the charge under the 2+/1+ peak, above the continuum background. Arrows indicate one, two, and three electron potential steps performed in chronoamperometry experiments; all jumps initiated at the MPC^{2+} charge state.

The peak currents in Figure 1 increase with successive dipping cycles. The number of MPC monolayers that they represent was estimated by integrating the area under the 2+/1+ current peak in the cyclic voltammograms. These results underestimate the total nanoparticle coverage, which comprises both the current peaks and the apparent background continuum current used as the baseline under the peaks. The peaks represent the dominant monodisperse fraction of nanoparticles, and the continuum the polydisperse remainder,[21] as discussed later. Results below confirm this.

Potential step chronoamperometry[15] was used to measure the rate of electron hopping (e.g., electron diffusion) through the MPC film. The current−time response relation appropriate for semi-infinite diffusion control of the electron hopping is (Cottrell equation)

$$I_T = nFAD_E^{1/2}C/\pi^{1/2}t^{1/2} \qquad (2)$$

where n is the change in core charge state, C is the MPC concentration[22] in the film (0.012 M), and the other symbols

(19) Hostetler, M. J.; Wingate, J. E.; Zhong, C.-J.; Harris, J. E.; Vachet, R. W.; Clark, M. R.; Londono, J. D.; Green, S. J.; Stokes, J. J.; Wignall, G. D.; Glish, G. L.; Porter, M. D.; Evans, N. D.; Murray, R. W. *Langmuir* **1998**, *14*, 17.

(20) (a) Fisher, M. C.; Wuelfing, W. P.; Zamborini, F. P.; Murray, R. W., manuscript in preparation. (b) Wuelfing, W. P.; Zamborini, F. P.; Templeton, A. C.; Wen, X.; Yoon, H.; Murray, R. W. *Chem. Mater.* **2001**, *13*, 87. (c) Determined by quartz crystal microbalance: Cliffel, D. E.; Murray, R. W., unpublished results, UNC-CH, 2000.

(21) The MPCs in the film that have a range of C_{CLU} values and thus ΔV values will yield an underlying featureless charging current. There will consequently be a range of charge states within the disperse fraction, but the *average* charge is probably near that of the more monodisperse fraction, since according to TEM core-size results, some MPCs will have larger and some smaller C_{CLU}.

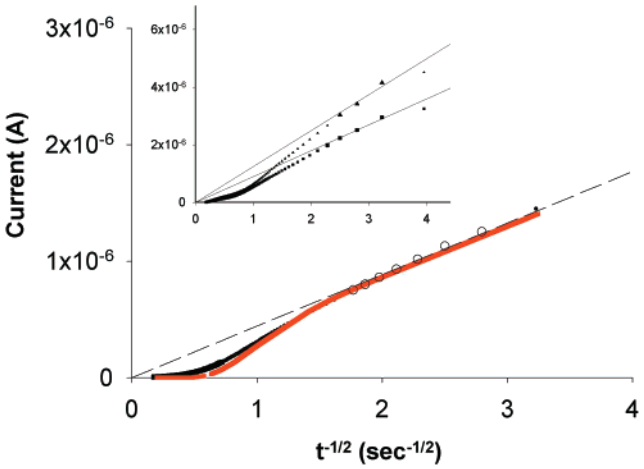

Figure 2. Current vs $t^{-1/2}$ curve for $n = 1$ potential step shown in Figure 1. Larger symbols are the points used in regression analysis, shown as a dashed line, which was forced through the origin as required by eq 2. The (red) solid line depicts the best fit to eq 3; see text for details. Inset: $n = 2$ (■) and $n = 3$ (▲) potential steps. Again, large symbols indicate the points used in regression analysis (dashed lines).

are as commonly known. The peak currents in the Figure 1 voltammograms lie at the "formal potentials" of the charge state changes[7] of the MPC cores; the valleys correspond to roughly monovalent charge states. Thus, at a potential of ca. +350 mV, nearly all of the MPCs in the film are in the 2+ charge state. The potential steps were valley-to-valley, i.e., between monovalent core charge state conditions. Stepping from a potential corresponding to a zero MPC core charge state (at the E_{PZC})[7b] to a value where the charge state is +1 corresponds to $n = 1$. The potential stepping illustrated in Figure 1A (see arrows) corresponds to changes of charge state from +2 to +1, 0, and −1, i.e., $n = 1$, 2, and 3, respectively, or vice versa.

Figure 2 shows current−time results of the $n = 1$ potential step illustrated in Figure 1A, plotted according to eq 2. Figure 2 (inset) gives the results for $n = 2$ and 3 potential steps. At all n values, at short times (right side of plot), the current vs $t^{-1/2}$ plot contains a linear segment that extrapolates to the origin, as required by the equation (see details in Figure 2 legend). At longer times, the current falls to lower values, which is expected from previous experience with redox polymers and which reflects the finite diffusion property of a limited film thickness. This is analyzed below. For the $n = 1$ potential step from the 2+ core double-layer charge to the adjacent 1+ state, the slope of the Cottrell plot is 4.4×10^{-6} C/s$^{1/2}$; using eq 2, this translates[22] to $D_E = 11 \times 10^{-8}$ cm^2/s, and using $\delta = 5.14$ nm in eq 1 gives a first-order rate constant $k_{HOP} = 2.5 \times 10^6$ s^{-1} and a self-exchange rate constant $k_{EX} = 2.1 \times 10^8$ M^{-1} s^{-1}.

Experiments such as that described in Figure 2 were done for a variety of MPC films and for $n = 1$ potential steps between various monovalent MPC core charge states, with results as shown in Table 1. There does not appear to be statistically significant variation in either D_E, k_{HOP}, or k_{EX} as a function of (a) the initial state of charge, (b) the direction of charging (positive or negative), or (c) film coverage. If such effects exist, these early experiments are insufficiently refined to isolate them.[23] For steps producing one-electron charge state changes,

Table 1. Electron Diffusion Coefficients and Electron-Transfer Rate Constants between Nanoparticles

Γ (mol/cm^2)	step	D_E ($\times 10^{-8}$ cm/s)[a]	k_{HOP} ($\times 10^6$ s^{-1})[b]	k_{EX} ($\times 10^8$ M^{-1} s^{-1})[c]
6.2×10^{-10} [d]	2+ → 1+	8.8	1.9	1.7
	1+ → 2+	5.9	1.3	1.8
9×10^{-10} [d]	2+ → 1+	11 (±5.1)[g]	2.5 (±0.81)	2.1 (±0.65)
	1+ → 2+	13 (±3.2)	2.9 (±0.92)	2.4 (±0.71)
	1+ → 0	12 (±5)	2.6 (±1.1)	2.1 (±0.91)
	0 → 1+	18 (±8)	3.9 (±1.8)	3.4(±1.5)
	0 → 1−	5.6 (±4.2)	1.2 (±0.93)	1.0 (±0.78)
	1− → 0	25 (±36)	5.7 (±8.0)	4.7 (±6.7)
	1− → 2−	2.5 (±1.6)	0.56 (±0.37)	0.46 (±0.31)
1.1×10^{-9} [d]	1+ → 2+	12	2.7	2.3
	0 → 1+	7.2	1.6	1.3
	1− → 0	4.7	1.1	0.89
6.2×10^{-10} [e]	2+ → 1−	7.2		
9×10^{-10} [e]	2+ → 0	13 (±2.8)		
	1+ → 1−	5.9		
	1− → 1+	10		
1.1×10^{-9} [e]	1+ → 1−	7.2		
9×10^{-10} [f]	2+ → 1+	11		
	2+ → 0	12		
	2+ → 1−	9.5		

[a] The [MPC] used in this calculation was 0.012 mol/L. [b] The core center−center separation distance (δ) used to calculate k_{HOP} was 5.14 nm. [c] The [MPC] concentration used to calculate k_{EX} was 0.012 mol/L. [d] Denotes single-electron changes. [e] Denotes multiple electron changes, i.e., $n = 2$ or $n = 3$. [f] Denotes one-, two-, and three-electron steps performed serially on the same film. [g] Uncertainties are standard deviations of results from typically three films of equal thickness.

the overall experimental values of D_E, k_{HOP}, and k_{EX} average to $10(\pm 5) \times 10^{-8}$ cm^2/s, $2(\pm 1) \times 10^6$ s^{-1}, and $2(\pm 1) \times 10^8$ M^{-1} s^{-1}, respectively.

Figure 2 (inset) also shows Cottrell plots for larger potential steps where the overall change in film double-layer charge is two and three electrons (i.e., $n = 2$ and 3). When one accounts for n, the slopes and D_E results from these plots are quite close to those found for the $n = 1$ experiment, i.e., 12×10^{-8} and 9.5×10^{-8} cm^2/s for $n = 2$ and 3, respectively, as compared to 11×10^{-8} cm^2/s for the $n = 1$ potential step on the same film. The $n > 1$ results are given in the lower part of Table 1. The D_E results for the $n = 1$ experiments are also generally in agreement with $n = 2$ and $n = 3$ experiments. We have not calculated k_{HOP} or k_{EX} rate constants from the latter results, since multielectron changes in double-layer charge within the film lead to sequential one-electron diffusion profiles bounded by zones of conproportionation reactions such as $MPC^{2+} + MPC^0 \rightarrow 2MPC^+$. The effective rate of charge transport is then (potentially) a hybrid of conproportionation and electron-hopping rates for individual $n = 1$ couples. (On the other hand, if we did calculate rate constants, the similarities of D_E values

(22) MPC concentration (0.012 M) was estimated on the basis of a cubic lattice relation $C = 1/\delta^3 N_A$, where N_A is Avogadro's number and δ is as defined in the text. The lattice repeat length $\delta = 5.14$ nm is based on summation of the average MPC core diameter (1.6 nm) and two fully extended MUA chain lengths (2 × 1.77 nm).

(23) The general absence of dependency on charge state supports our view that migration effects associated with (a) charge-compensating counterion movement or (b) intrafilm electrical gradients are not significant. (A) For electroneutrality, double-layer charging must be accompanied by counterion migration through the multilayer. Whether this constitutes an influx of electrolyte anions or efflux of film cations is unknown, but the stability of the observed voltammetry suggests the former. (B) Theory[24,25] for intrafilm electrical gradients in redox polymer films, present when electron mobility exceeds ion mobility, shows that such gradients can inflate the measured values of k_{HOP} and k_{EX}. Both (a) and (b) should depend on the charging direction, but no such effect is obvious, within experimental uncertainty, in the D_E results. Measurement of counterion as well as electron diffusivity[26,27] also allows inspection of this problem.

(24) Facci, J. S.; Schmehl, R. H.; Murray, R. W. *J. Am. Chem. Soc.* **1982**, *104*, 4960.

(25) Andrieux, C. P.; Saveant, J.-M. *J. Phys. Chem.* **1988**, *92*, 6761.

(26) Surridge, N. A.; Zvanut, E.; Keene, F. R.; Sosnoff, C. S.; Silver, M.; Murray, R. W. *J. Phys. Chem.* **1992**, *96*, 962.

(27) Surridge, N. A.; Sosnoff, C. S.; Schmehl, R.; Facci, J. S.; Murray, R. W. *J. Phys. Chem.* **1994**, *98*, 917.

show that they would be much the same as the $n = 1$ results, which implies that conproportionation reactions are quite rapid.)

The nearly 10^6 s^{-1} average rate constant in Table 1 for the change in the core double-layer charge is very large and exceeds the most rapid electron-hopping rates that we have encountered[24] in redox polymers. We envision that the electron-hopping process is a core edge-to-edge tunneling reaction through the intervening monolayer and linking structure. Seeking examples that produce rate constants of the same 10^6 s^{-1} magnitude, we present two comparisons of literature data to this rate constant. The first example is based on the dynamics[28,29] of electron transfers between Au electrodes and ferrocene units that are separated from the electrode surface by well-defined methylene linker chains. A chain length of five methylene units linking the electrode to ferrocene would give a 10^6 s^{-1} rate constant. The second example is based on the solid-state conductivity[9] of mixed-valent (0/1+) hexanethiolate Au_{140} MPCs, which exhibit (30 °C) an electron-hopping rate constant of 10^8 s^{-1}. Extrapolating this rate constant using the estimated[9] electronic coupling factor $\beta \approx 0.8$ Å^{-1}, one anticipates that an edge-to-edge core spacing equivalent to about 13 methylene units would have displayed a solid-state electron-hopping rate constant of about 10^6 s^{-1}.

The MPC linking structure is shown in more detail, and roughly to scale, in Scheme 2. The linking structure has an overall length of 27 atoms, including 22 methylene units. The MPC metal core-to-metal core electron-transfer reaction obviously behaves as though it is intrinsically much faster than a Au metal-to-ferrocene reaction (a possible consequence of the MPC cores being shrouded in a low-dielectric medium, producing a low reorganization energy[30]). Second, the reaction may occur through a shorter tunneling bridge (or multiple bridges) than that shown in Scheme 2. The linker chains in the MPC films are flexible, being buttressed only by the shorter hexanethiolate chains in the MPC mixed monolayer. Added chain freedom is associated with the small curvature radius of the MPC core. If the thermal motion time scale of MPCs within the linker lattice approaches that of the electron transfers, the electron-hopping reaction might occur at much shorter distances[31] than in Scheme 2. For example, thermal motion contact bringing together the heads of the hexanethiolate monolayers, i.e., $-(CH_2)_5CH_3/CH_3(CH_2)_5-$, would amount to a roughly 12 methylene unit MPC core edge-to-edge separation. This not only is a much shorter tunneling bridge but also is close to the 13 methylene unit spacing that, in the solid-state MPCs, gives a 10^6 s^{-1} rate constant. We have to consider the obvious difference between these two experiments, including the lack of solvent in one. (Recent electronic conductivity measurements on carboxylate/metal ion/carboxylate films reveal that films are less conductive when bathed in solvent liquid or vapor (dichloromethane) as opposed to dry air,[32] an effect preliminarily assigned to film swelling and an associated increase in δ.) Testing these views obviously will require further experiments, notably aimed at adjusting the linker and MPC monolayer chain length. Both are in principle possible, but must overcome the synthetic challenge[4] of preparing monodisperse MPCs with longer chain lengths, and of retaining adequate ionic mobility within a more tightly linked MPC film.

We return to the finite diffusion characteristic of the potential step experiments noted above (the drop-off of current in the Figure 2 Cottrell plots). At short times, the electron diffusion geometry is "semi-infinite", and the current vs $t^{-1/2}$ curve is described by the Cottrell equation (eq 2). At longer times, the diffusion profile of MPCs whose double-layer charge has been changed reaches the outer boundary of the MPC film, beyond which there are no further MPC sites, and the current then decays with time. This situation is described by[14,15]

$$i(t) = nFAD_E^{1/2}C/\pi^{1/2}t^{1/2}[\Sigma(-1)^k(\exp[-k^2d^2/D_Et] - \exp[-(k+1)^2d^2/D_Et])] \quad (3)$$

where d is the film thickness (cm) and the other symbols are as in eq 2. (This relation reduces to eq 2 at short time.) Equation 3 reasonably predicts the decrease in current at long times, as shown by the solid fitted line (colored lower curve) in Figure 2. The solid line also fits the short-time segment in Figure 2. The plot of eq 3 uses the concentration of MPCs in the film (1.2×10^{-5} mol/cm^3) and the value of D_E (11×10^{-8} cm^2/s) determined from the short-time fit to eq 2, noted above.

A value of the film thickness d has to be input into the plot of eq 3 in Figure 2. The eq 3 plot is rather sensitive to d, so adjusting it for a best fit is a good route to determining its real dimension. An initial estimate of $d = 7.5 \times 10^{-5}$ cm was based on the ratio Γ_T/C, where Γ_T is estimated from the charge under the cyclic voltammetry peaks (using the underlying featureless cyclic voltammetry charging current envelope as baseline). To achieve a good fit in the eq 3 comparison in Figure 2 required a substantially larger value, $d = 4.3 \times 10^{-4}$ cm. This larger d reflects, we believe, the portion of the film that generates the featureless cyclic voltammetry charging current below the charging peaks. Estimating film thickness by using the *total* current at the current peak in the equation for a thin-layer cell[15] gives in fact an apparent thickness within 20% of that found in Figure 2. The large featureless charging current is not present before MPCs are attached to the electrode surface and grows in more or less linear concert with the size of the cyclic voltammetry current peaks (Figure 1B). The featureless charging current arises from the core size polydisperse portion of the MPCs that are attached to the electrode; the voltammetric peak that rides above it measures in contrast the population of MPCs that have a uniform core size and the value of the double-layer capacitance C_{CLU}. That population evidently is less than 50% of the total for the MPC samples used here. This result is consistent with transmission electron microscopy (TEM) histograms[4] of core size. Fits of eq 3 to results of $n = 2$ and 3 potential step experiments produced reasonably good fits, as did others[33] for $n = 1$ experiments and for films of differing thickness. The d value providing the best fit was always larger than the value estimated from the charge under the CV current peak.

In summary, the D_E, k_{HOP}, and k_{EX} results of this report provide new information on the electron-transfer dynamics of

(28) Chidsey, C. E. D. *Science* **1991**, *251*, 919.

(29) Smalley, J. F.; Feldberg, S. W.; Chidsey, C. E. D.; Linford, M. R.; Newton, M. D.; Liu, Y.-P *J. Phys. Chem.* **1995**, *99*, 13141.

(30) (a) An outer-sphere reorganization energy (λ_o) of ca. 4 kJ/mol (0.04 eV) was estimated from[30b] $\lambda_o = N_A e^2/4\pi\epsilon_0(1/2a + 1/2a - 1/\delta_R)(1/\epsilon_{op} - 1/\epsilon_s)$, where a is the reactant radius (taken as 2.57 nm), δ_R is the center−center core separation at the time of the reaction, and ϵ_{op} (taken as 2.09) and ϵ_s (taken as 3.0) are the optical and static dielectric constants of the monolayer, respectively. This λ_o may be too high, since the calculation assumed that $\delta_R = \delta = 5.14$ nm, and it may be that $\delta_R < \delta$. (b) Marcus, R. A.; Sutin, N. *Biochim. Biophys. Acta* **1985**, 811, 265.

(31) In this discussion one must remember that δ, the overall diffusive hopping distance, is a summation of thermal translation distance and tunneling barrier length at reaction.

(32) Zamborini, F. P.; Murray, R. W., unpublished results.

(33) A few films produced Cottrell plots (Figure S-1) that, in contrast to Figure 2, exhibited current decays in the finite diffusion segment of the plot that were substantially elongated and which were not well-fit by eq 3. We believe this behavior reflects some nonuniformity in the film, either in its actual thickness or in its charge-transporting characteristic.

metallic nanoparticles. This information is a stepping stone to understanding fully the molecular influences and/or controls on electron-transfer reactions in these systems. We have begun experiments designed to probe the questions that these experiments have generated.

Not only the length of the linker chain but also its flexibility are obvious experimental directions, to better define the core-to-core separation distance at reaction. We also plan to investigate the influence, if any, of the linker chain metal ion on the rate of electron transfer within the film. The role of the metal ion beyond its function as a linker is unknown and deserves further attention. These experiments are aimed at the controlled manipulation of D_E and subsequently k_{HOP}, resulting in the ability to design nanoparticle assemblies with useful electronic properties.

Acknowledgment. This research was supported in part by grants from the National Science Foundation and the Office of Naval Research.

Supporting Information Available: Figure S-1, the Cottrell plots described in footnote 33 (PDF). This material is available free of charge via the Internet at http://pubs.acs.org.

JA0106826